JOURNAL OF MATERIALS SCIENCE **36** (2001) 1665–1670

Cryogenic properties of Si-Ti-C-O fibre-bonded ceramic using satin weave

K. MATSUNAGA, T. ISHIKAWA, S. KAJII, T. HOGAMI
Ube Research Laboratory, Ube Industries Ltd, Ube City, Yamaguchi Prefecture, 755-8633, Japan
E-mail: 24613u@ube-ind.co.jp

Mechanical and thermophysical characteristics of Si-Ti-C-O fibre-bonded ceramic produced by hot-pressing the laminated material of oxidized satin-woven Si-Ti-C-O fibre have been investigated at room and cryogenic temperatures. The fibre element (diameter: 8 μm, fibre volume fraction: 85 ± 1%) constructing the Si-Ti-C-O fibre-bonded ceramic showed a close-packed structure of the oxidized Si-Ti-C-O fibre mainly composed of fine SiC crystals, amorphous SiO_2-based phase and turbostratic carbon. The Si-Ti-C-O fibre-bonded ceramic with lightweight (density: 2.45×10^3 kg/m^3) and low porosity ($<$1 vol%) showed a markedly higher fracture energy (notched, cross-plied specimen: approximately 10 kJ/m^2) and lower thermal conductivity (1/10 the value of stainless steel). The reason why the fibre-bonded ceramic showed such a low thermal conductivity in spite of very high thermal conductivity of a pure SiC and carbon could be attributed to the complicated microstructure of Si-Ti-C-O fibre-bonded ceramics.

1. Introduction

Ceramic matrix composites (CMCs) reinforced with continuous fibres have been identified as the most promising candidate of thermostructural materials, because they guarantee a high heat-resistance and an excellent fracture toughness [1–3]. Moreover, the application of monolithic ceramics and CMCs in cryogenic field has been recently examined as a thermal insulator [4].

Several years ago research scientists of the Ube industries Ltd have developed a unique Si-Ti-C-O fibre-bonded ceramic that was lightweight and had excellent oxidation resistance (up to 1500 °C) and high fracture energy [5, 6]. The Si-Ti-C-O fibre-bonded ceramic shows a close-packed structure of raw fibres, with the interstices between the fibres perfectly filled with both the oxide material, which initially covered the raw fibres, and very fine TiC particles ($<$50 nm) uniformity dispersed in this oxide material [7]. Moreover a thin interfacial carbon layer (thickness: $\sim$15 nm) which is turbostratic in structure exists around all the foregoing fibres. Authors have so far investigated about the high-temperature properties of Si-Ti-C-O fibre-bonded ceramic with such microstructure [8–10]. For example, it was found that the initial strength of Si-Ti-C-O fibre-bonded ceramic was retained up to 1400°C in air and after heat-treatment up to 1500°C in air for 1000 hours. These favourable properties make the Si-Ti-C-O fibre-bonded ceramic suited for high-temperature structural materials that require high efficiency and functionality. As noted above, although several studies have been performed on mechanical properties of Si-Ti-C-O fibre-bonded ceramic at room and high temperatures, little information about cryogenic properties has been forthcoming. Moreover, the interior structure of fibre element comprising Si-Ti-C-O fibre-bonded ceramic composites has not been also made clear.

In this work, the cryogenic properties of Si-Ti-C-O fibre-bonded ceramic and the microscopic structure of the fibre element were also investigated.

2. Experimental procedure

2.1. Material

The starting material used in this study was Si-Ti-C-O fibre* which contained non-stoichiometric excess of carbon of SiC and oxygen of 12 mass %. At the first step, the single Si-Ti-C-O fibre [11] (diameter: 8 ± 0.5 μm) bundles were oxidized in ambient air at 1000 °C for 20 h resulting in an oxide layer of about 300 nm in thickness on the fibre surface. The eight-harness satin weave fabric was prepared from the pre-oxidized Si-Ti-C-O fibres. A preform was then prepared by laminating the satin weaves made of the pre-oxidized Si-Ti-C-O fibre. The Si-Ti-C-O fibre-bonded ceramic was produced by hot-pressing the preform in argon atmosphere at 1750 °C and 40 MPa for 1 hour using a hot-press machine.† The density, fibre volume fraction, and porosity of the material were $2.45 \pm 0.05 \times 10^3$ kg/m^3, 85 ± 1 vol%, and less than 1 vol%, respectively.

* Tyranno fibre®, LoxM grade, Ube Industries Ltd., Japan.

† Model EVHP-R-50, Fujidenpa Co., Ltd., Japan.

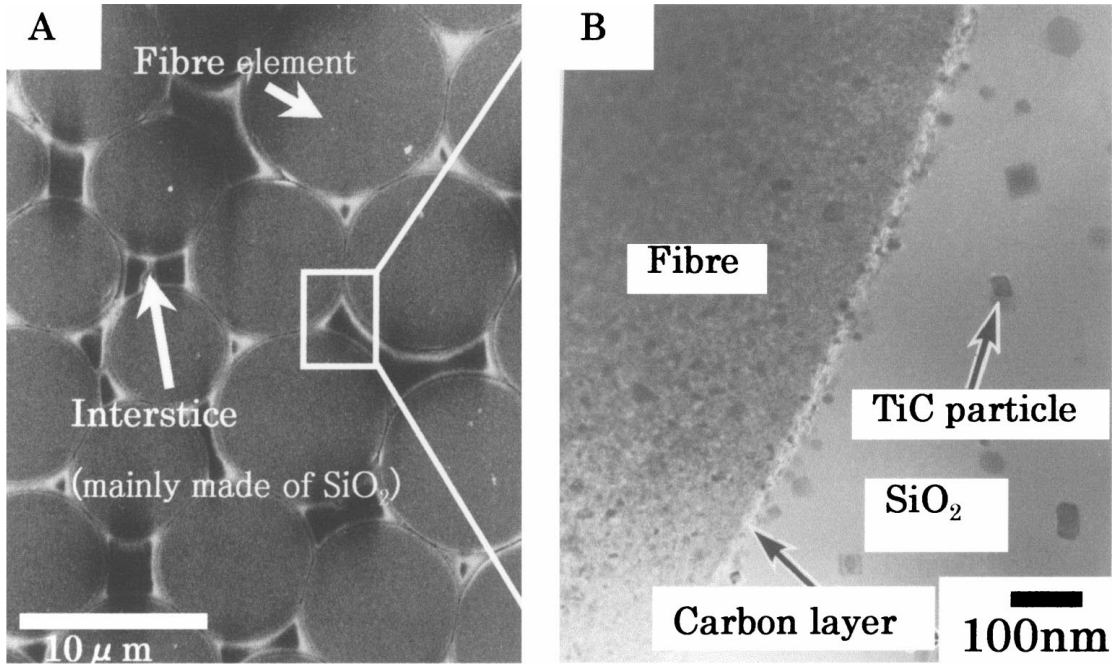

Figure 1 SEM and TEM micrographs showing cross section of Si-Ti-C-O fibre-bonded ceramic; (a) a scanning electron microscope (SEM) micrograph of Si-Ti-C-O fibre-bonded ceramic; (b) a transmission electron microscope (TEM) micrograph near the fibre-SiO_2 interface of Si-Ti-C-O fibre-bonded ceramic.

2.2. Measurement

The microstructure of the fibre element constructing Si-Ti-C-O fibre-bonded ceramic was observed by a high-resolution transmission electron microscopy[‡] operating at an acceleration voltage of 200 kV.

The four point bending test was carried out at room temperature and −190°C[§] at a crosshead speed of 0.5 mm min^{-1} using the unnotched specimen with a size of 4 mm (width) by 3 mm (thickness) by 40 mm(length), following JIS R 1601 method for the other conditions. The loading and supporting spans were 10 mm and 30 mm, respectively. The fracture energy was measured by the Charpy impact-testing machine[¶] using the notched specimen with a size of 10 mm (width) by 6 mm (thickness) by 80 mm (length) at room temperature and −140°C,* following JIS K 7077 method for the other conditions. The depth of the notch is 3 mm. The fracture energy was calculated using

$$\text{Fracture energy} = E/\{2B(W - A)\} \qquad (1)$$

where E is the absorbed energy, B the width of the specimen, W the thickness of the specimen and A the depth of the notch. For comparison, those mechanical characteristics of zirconium oxide (ZrO_2), which is one of the candidates for strong insulating ceramic used in the cryogenic field, was also evaluated. The fracture surface of Si-Ti-C-O fibre-bonded ceramic was examined by a scanning electron microscope[†] at an acceleration voltage of 10 kV.

Estimation of specific heat (C_p) using the specimen with a size of 10 mm (diameter) by 2 mm (thickness) was carried out at room temperature, −100°C, and −150°C[‡] by differential thermal analysis. The thermal conductivity (γ) was calculated using

$$\gamma = \alpha\rho C_p \qquad (2)$$

where α is the thermal diffusivity which it is determined by the laser flash method, and ρ the density of Si-Ti-C-O fibre-bonded ceramic.

3. Results and discussion

3.1. Microstructure

Figs 1 and 2 shows SEM and TEM micrographs, and TEM image of the Si-Ti-C-O fibre-bonded ceramic, respectively. The Si-Ti-C-O fibre-bonded ceramic showed a close-packed structure of round columnar fibre (see in Fig. 1a) and the interstices among fibres were completely filled with silicon oxide, in which very fine TiC particles (<50 nm diameter) were uniformly dispersed (see in Fig. 1b). Moreover, an interfacial carbon layer (10–20 nm) was uniformly formed around all the fibres. In this study, the microstructure of the fibre element comprising the Si-Ti-C-O fibre-bonded ceramic was also observed in detail. In the fibre element, very fine SiC crystals, partly covered with a thin carbon layer (carbon ribbon), were found to be in coherent existence (see in Fig. 2). Through selected-area electron diffraction of the fibre element, it was found that the carbon ribbon was turbostratic in structure and the SiC crystal showed random orientation. Furthermore, a small amount of amorphous phase was observed among the SiC crystals and carbon ribbon. Judging from these observations, the

‡ Model JEM-2010, Jeol-Technics Co., Ltd., Tokyo, Japan.

§ This value shows the temperature of specimen in liquid nitrogen.

¶ Model CHARAC, Yonekura Seisakusyo Ltd., Japan. (1.16 kg hammer weight, 150° raising angle of the hammer, 188 mm length of the hammer).

* This value shows the temperature of specimen that set on the Charpy impact-testing machine after treatment in liquid nitrogen.

† Model JST-T220, Jeol-Technics Co., Ltd., Tokyo, Japan.

‡ This value is lower limit of equipment.

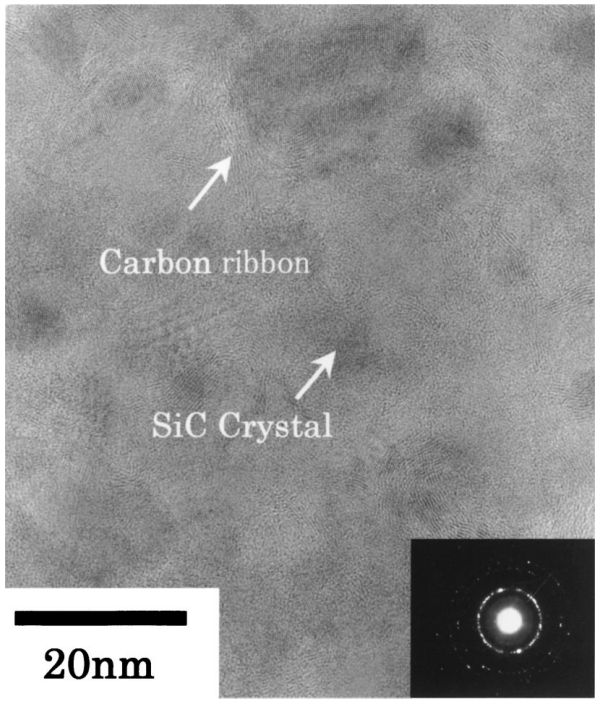

Figure 2 The enlarged TEM micrograph showing cross section of Si-Ti-C-O fibre-bonded ceramic.

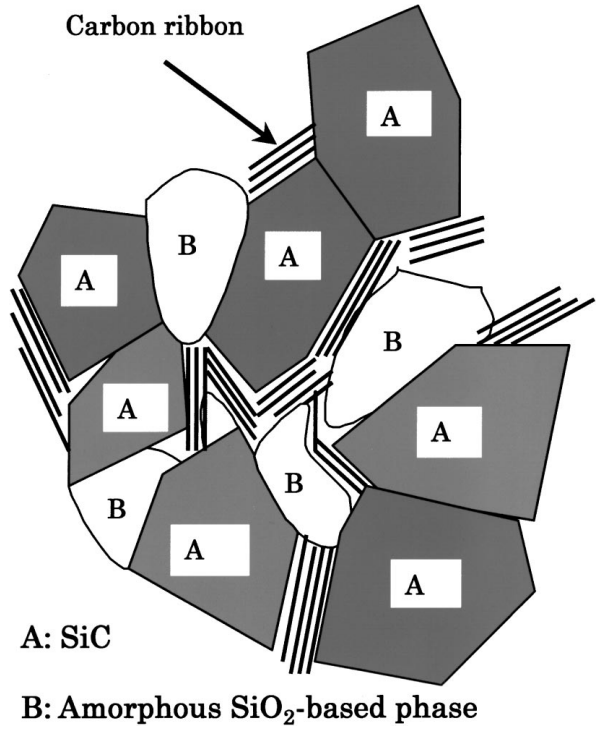

Figure 3 Schematic representation showing microstructure of the fibre element.

Si-Ti-C-O fibre-bonded ceramic is comprised of the following elements.

1. Fibre element (about 85 vol%) composed of a mixture of three structural units. (fine SiC crystals, thin carbon ribbon and amorphous SiO_2-based phase)
2. Interfacial carbon layer around every fibre.
3. SiO_2-based oxide matrix (about 12 vol%) including TiC particles which exist at the interstices among fibres.

Fig. 3 shows the schematic representation of microstructure of the fibre element comprising the Si-Ti-C-O fibre-bonded ceramic.

3.2. Mechanical characteristics

Figs 4 and 5 show typical flexural stress-displacement curves and the four-point flexural strength of Si-Ti-C-O fibre-bonded ceramic at room temperature and −190°C, respectively. The Si-Ti-C-O fibre-bonded ceramic showed non-linear fracture behaviour even in a cryogenic environment. Furthermore, the strength at −190°C was larger than at room temperature. However, the difference of test temperatures has neither significant influence on the flexural stress-displacement curves nor on the fracture surfaces. On both fractures surfaces a large amount of fibre pull-out could be observed. Fig. 6 shows the typical fracture surface after the bending test at −190°C.

The fracture energy of Si-Ti-C-O fibre-bonded ceramic measured by the Charpy impact-testing machine using the notched specimen at room temperature and −140°C was shown in Fig. 7 together with that of zirconium oxide $(ZrO_2) \cdot ZrO_2$ is one of the candidates for strong insulating ceramic used in the cryo-

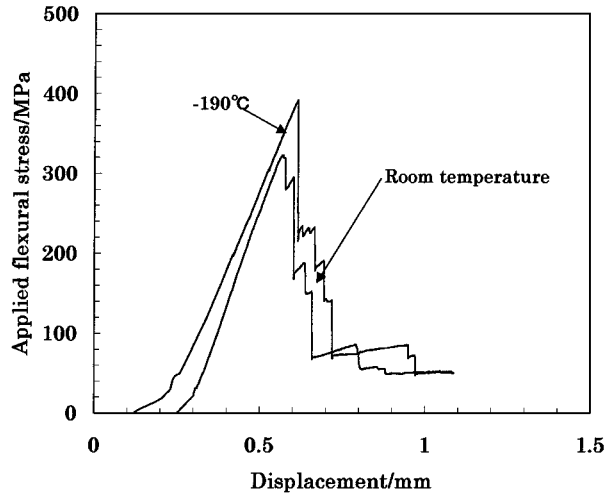

Figure 4 Typical bending stress-displacement curve of Si-Ti-C-O fibre-bonded ceramic tested at room temperature and −190°C.

genic field, and it is well known as a tough ceramic with higher fracture energy compared with other representative ceramic. The fracture energy of the Si-Ti-C-O fibre-bonded ceramic was very high compared with the ZrO_2. The fractured test specimens of both Si-Ti-C-O fibre-bonded ceramic and ZrO_2 after testing at −140°C are shown in Fig. 8. The composite specimen shows fibrous, "woody" fracture behavior, whereas the monolithic specimen shows brittle fracture behaviour. It has been found that this "woody" fracture behaviour of the Si-Ti-C-O fibre-bonded ceramic was caused by the existence of the interfacial carbon layer around the fibres. The authors have up until now investigated only the high-temperature properties of Si-Ti-C-O fibre-bonded ceramic [5–9]. From this information, it has been found that the mechanical

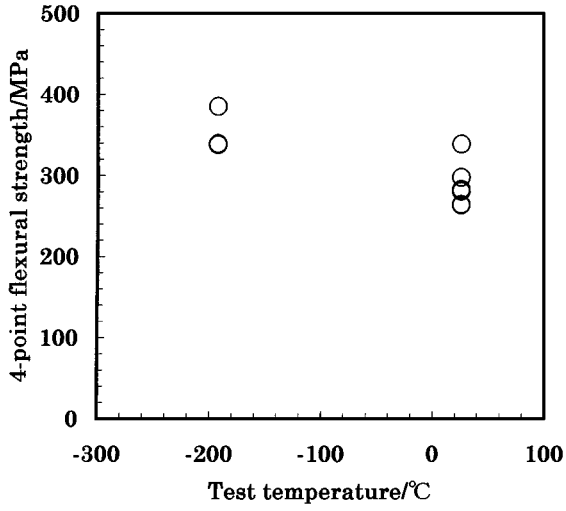

Figure 5 Relation between test temperature and four-point bending strength of Si-Ti-C-O fibre-bonded ceramic.

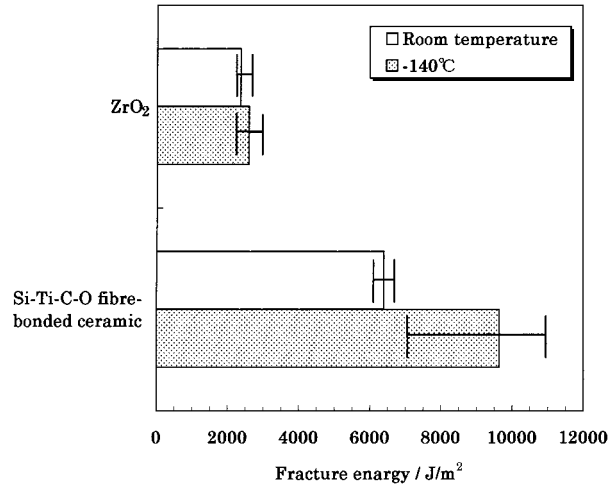

Figure 7 Relation between test temperature and impact fracture energy of Si-Ti-C-O fibre-bonded ceramic, together with that of zirconium oxide.

properties of Si-Ti-C-O fibre-bonded ceramic retain the strength at room temperature even when heated to 1400°C. From the current work, it was found that Si-Ti-C-O fibre-bonded ceramic showed excellent mechanical properties at wide-ranging temperatures from cryogenic field to ultra-high temperatures.

Incidentally, the mechanical properties at a cryogenic temperature were greater than at room temperature, whereas fracture morphology was not altered by change of temperature. In other words, the change of interfacial characteristics at fibre-fibre and/or fibre-matrix was not the main cause of the increase in the mechanical

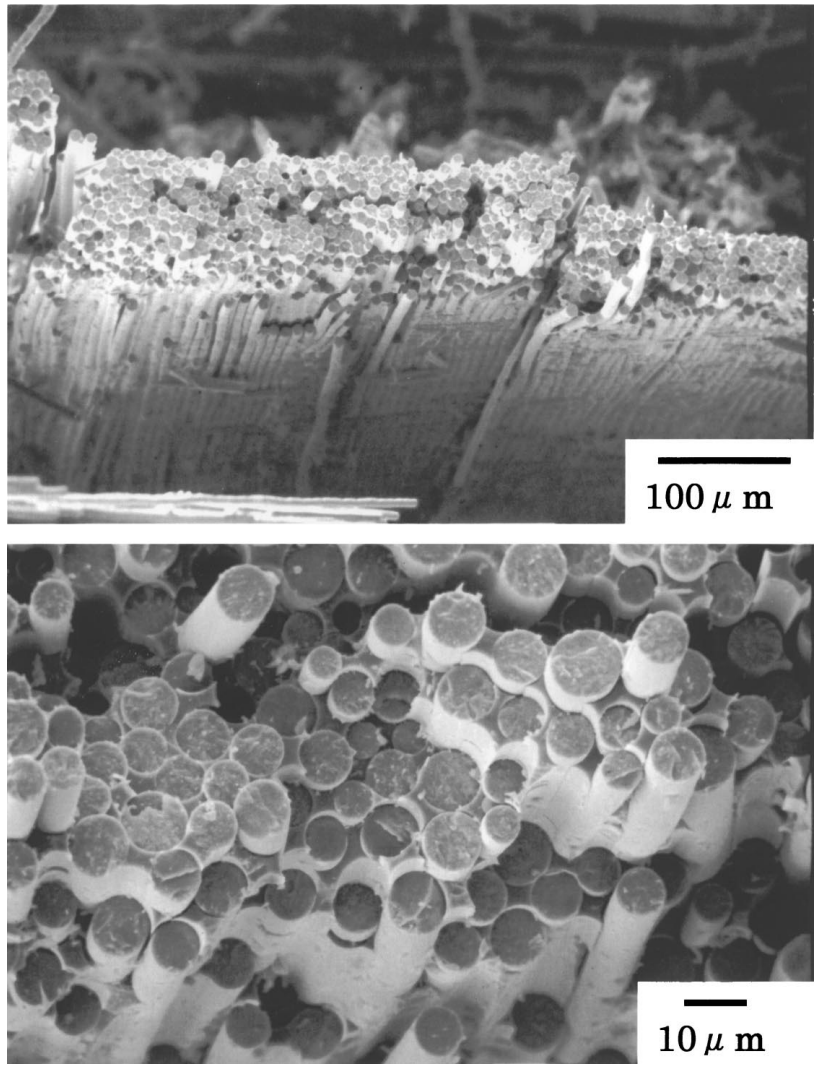

Figure 6 SEM micrograph showing bending fracture morphology of Si-Ti-C-O fibre-bonded ceramic tested at −190°C.

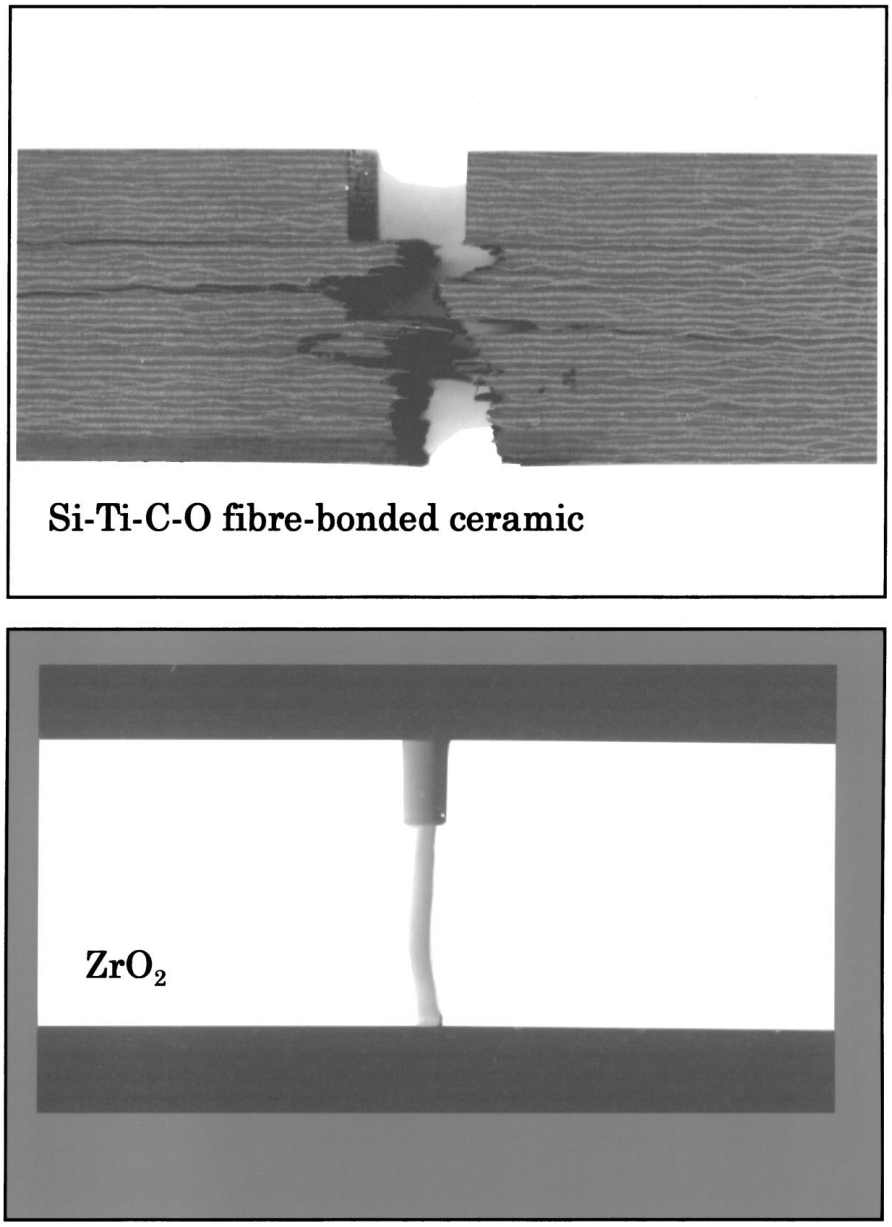

Figure 8 Specimens of Si-Ti-C-O fibre-bonded ceramic and ZrO_2 after the test of fracture energy using the charpy impact testing machine at -140°C.

properties at cryogenic temperature. The reason why the remarkable increase in the mechanical properties occurs in a cryogenic field has not been clarified, but it has been assumed that some changes in the thermal activation process of the fracture are involved.

3.3. Thermophysical characteristics

The thermal conductivity of Si-Ti-C-O fibre-bonded ceramic is shown in Fig. 9 along with that of other materials, including a stainless steel (Stainless steel, density: 7.8×10^3 kg/m^3). As can be seen from this figure, the thermal conductivity of Si-Ti-C-O fibre-bonded ceramic is as low as that of ZrO_2. Furthermore, the thermal conductivity of Si-Ti-C-O fibre-bonded ceramic is about a tenth of that of Stainless steel. What is better, the lower the temperature, the lower the thermal conductivity becomes in a super cryogenic field. The Si-Ti-C-O fibre-bonded ceramic is lightweight, has higher fracture energy and has lower thermal conductivity giving it great possibilities as a replacement of heavy metals used in the cryogenic field.

Heat conduction in the ceramic without translation of free conduction electrons is due primarily to the mechanical interaction between molecules (i.e., lattice vibrations). Because lattice vibrations can be treated as phonons, thermal transport in solids can be regarded as energy transport in phonon, and the mean-free-path concept from the kinetic theory of gases is applicable [12]. Through the kinetic theory of gases, the following equation has been proposed.

$$K = 1/3\, C_v V L \tag{3}$$

Where K is the thermal conductivity, C_v is the specific heat capacity, V is the propagation velocity of carrier, and L is the mean free path. Fig. 10 shows the thermal conductivity and the specific heat of Si-Ti-C-O fibre-bonded ceramic at the temperatures between -140°C and room temperature. The variation of the thermal conductivity was approximately consistent with the specific heat. The reason why the thermal conductivity decreased with decreasing temperature could be attributed to the decrease in the specific heat. In other

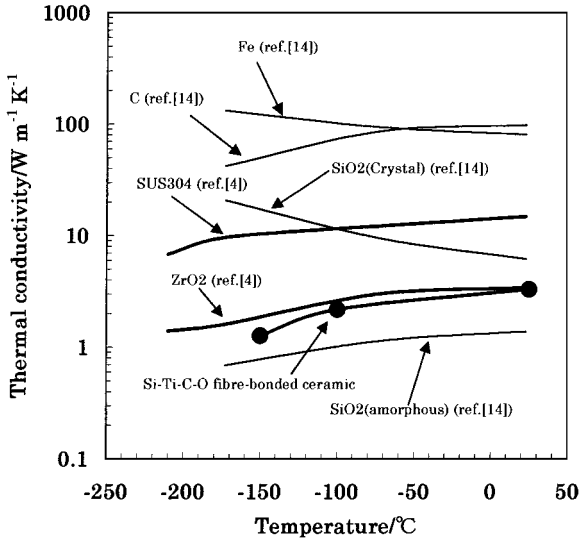

Figure 9 Temperature-dependence of thermal conductivity of Si-Ti-C-O fibre-bonded ceramic in the direction through the thickness along with those of other materials including ZrO_2 and SUS.

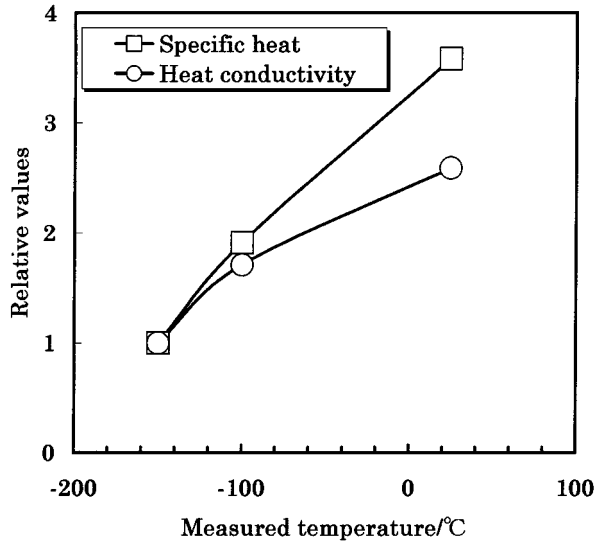

Figure 10 Temperature-dependence of thermal conductivity and the specific heat of Si-Ti-C-O fibre-bonded ceramic.

words, the number of the phonon was due to decrease with decreasing temperature.

The thermal conductivity of Si-Ti-C-O fibre-bonded ceramic is considered less than that other materials. In general, impurities in the solids cause a significant decrease in thermal conductivity. Both small grain size and the existence of many grain boundaries in the solid also reduce the thermal conductivity because they shorten the mean-free-path [13]. Therefore, for SiC fibre-bonded ceramic, it is concluded that (i) the existence of many grain boundaries in the fibre element and (ii) amorphous SiO_2-based phase which exists in the fibre element and at the interstices among fibres play an important role in the reduction of the thermal conductivity.

4. Summary and conclusion

The mechanical and the thermophysical characteristics, and the microstructure of Si-Ti-C-O fibre-bonded ceramic produced by hot-pressing an oxidized satin-woven Si-Ti-C-O fibre were examined at the temperature between room and cryogenic temperatures. The results are summarised as follows.

1. The fibre element constructing the Si-Ti-C-O fibre-bonded ceramic was mainly consisted of fine SiC crystals, amorphous SiO_2-based phase and turbostratic carbon.
2. The Si-Ti-C-O fibre-bonded ceramic also retained high fracture energy at a cryogenic temperature.
3. It was clarified that the thermal conductivity of Si-Ti-C-O fibre-bonded ceramic was very low and this material would be usable as a shock-resistant insulating wall in the cryogenic field.

For reasons mentioned above, the Si-Ti-C-O fibre-bonded ceramic make it very attractive for replacement of brittle ceramic or heavy metal components at wide-ranging temperatures from cryogenic fields to super high temperatures.

References

1. C. F. WINDISCH JR., C. H. HENAGER JR., G. D. SPRINGER and R. H. JONES, *J. Am. Ceram. Soc.* **80**(3) (1997) 567.
2. H. WANG and R. N. SINGH, *J. Mater. Sci.* **32** (1997) 3305.
3. M. G. JENKINS and M. D. MELLO, *Materials and Manufacturing Processes* **11**(1) (1996) 99.
4. S. NISHIJIMA, *Journal of the Japan Society of Powder and Powder Metallurgy* **41**(10) (1994) 1209.
5. T. ISHIKAWA, S. KAJII, K. MATSUNAGA, T. HOGAMI and Y. KOHTOKU, *J. Mater. Sci.* **30** (1995) 6218.
6. S. KAJII, T. ISHIKAWA, K. MATSUNAGA and Y. KOHTOKU, *Advanced Performance Materials* **1** (1994) 145.
7. T. ISHIKAWA, S. KAJII, Y. KOHTOKU and T. YAMAMURA, *Ceramic Engineering and Science Proceedings* **18**(3) (1997) 771.
8. K. MATSUNAGA, T. ISHIKAWA, S. KAJII, T. HOGAMI and Y. KOHTOKU, *J. Ceram. Sci. Japan Int. Edition* **103** (1995) 292.
9. *Idem., J. Japan Inst. Metals* **60**(12) (1996) 1236.
10. *Idem., J. Mater. Sci.* **34** (1999) 1505.
11. T. YAMAMURA, T. ISHIKAWA, M. SHIBUYA, T. HISAYUKI and K. OKAMURA, *ibid.* **23** (1988) 2589.
12. C. L. TIEN and A. J. STRETTON, "Heat Mass Transfer Refring. Cryog." (International Symposium on Heat and Mass Transfer in Refrigeration and Cryogenics, Dubrovnik, 1987) p. 3.
13. F. R. CHARVAT and W. D. KINGERY, *J. Am. Ceram. Soc.* **40**(9) (1957) 306.
14. R. TAMAMUSI, in "Kagaku Binran II," edited by (Chemical Society of Japan, Maruzen Press, 1993) p. II-66.

Received 11 April
and accepted 18 August 2000